THE JOURNAL OF BIOLOGICAL CHEMISTRY VOL. 284, NO. 48, pp. 33400–33408, November 27, 2009

Depletion of Vitamin E Increases Amyloid β Accumulation by Decreasing Its Clearances from Brain and Blood in a Mouse Model of Alzheimer Disease*[S]

Received for publication, August 9, 2009 Published, JBC Papers in Press, August 13, 2009, DOI 10.1074/jbc.M109.054056

Yoichiro Nishida[‡], Shingo Ito[§], Sumio Ohtsuki[§], Naoki Yamamoto[¶], Tsubura Takahashi[‡], Nobuhisa Iwata[‖], Kou-ichi Jishage[**], Hiromi Yamada[‡], Hiroki Sasaguri[‡], Shigefumi Yokota[‡], Wenying Piao[‡], Hiroyuki Tomimitsu[‡], Takaomi C. Saido[‖], Katsuhiko Yanagisawa[¶], Tetsuya Terasaki[§], Hidehiro Mizusawa[‡], and Takanori Yokota[‡1]

From the [‡]Department of Neurology and Neurological Science, Graduate School, Tokyo Medical and Dental University, 1-5-45 Yushima, Bunkyo-ku, Tokyo 113-8519, the [§]Department of Molecular Biopharmacy and Genetics, Graduate School of Pharmaceutical Sciences, Tohoku University, Aoba, Aramaki, Aoba-ku, Sendai, Miyagi 980-8578, the [¶]National Institute for Longevity Sciences, National Center for Geriatrics and Gerontology, 36-3 Gengo, Morioka, Obu, Aichi 474-8522, the [‖]Laboratory for Proteolytic Neuroscience, RIKEN Brain Science Institute, 2-1 Hirosawa, Wako-shi, Saitama 351-0198, and the [**]Chugai Research Institute for Medical Science, Inc., Gotenba, Shizuoka 412-8513, Japan

Increased oxidative damage is a prominent and early feature in Alzheimer disease. We previously crossed Alzheimer disease transgenic (*APPsw*) model mice with α-tocopherol transfer protein knock-out (*Ttpa*$^{-/-}$) mice in which lipid peroxidation in the brain was significantly increased. The resulting double-mutant (*Ttpa*$^{-/-}$*APPsw*) mice showed increased amyloid β (Aβ) deposits in the brain, which was ameliorated with α-tocopherol supplementation. To investigate the mechanism of the increased Aβ accumulation, we here studied generation, degradation, aggregation, and efflux of Aβ in the mice. The clearance of intracerebral-microinjected ^{125}I-Aβ$_{1-40}$ from brain was decreased in *Ttpa*$^{-/-}$ mice to be compared with wild-type mice, whereas the generation of Aβ was not increased in *Ttpa*$^{-/-}$*APPsw* mice. The activity of an Aβ-degrading enzyme, neprilysin, did not decrease, but the expression level of insulin-degrading enzyme was markedly decreased in *Ttpa*$^{-/-}$ mouse brain. In contrast, Aβ aggregation was accelerated in *Ttpa*$^{-/-}$ mouse brains compared with wild-type brains, and well known molecules involved in Aβ transport from brain to blood, low density lipoprotein receptor-related protein-1 (LRP-1) and p-glycoprotein, were up-regulated in the small vascular fraction of *Ttpa*$^{-/-}$ mouse brains. Moreover, the disappearance of intravenously administered ^{125}I-Aβ$_{1-40}$ was decreased in *Ttpa*$^{-/-}$ mice with reduced translocation of LRP-1 in the hepatocytes. These results suggest that lipid peroxidation due to depletion of α-tocopherol impairs Aβ clearances from the brain and from the blood, possibly causing increased Aβ accumulation in *Ttpa*$^{-/-}$*APPsw* mouse brain and plasma.

The accumulation of amyloid β (Aβ)[2] is the primary pathological event driving neurodegeneration in Alzheimer disease (AD). Support of this hypothesis is based on genetic evidence from cases of familial AD with β-amyloid precursor protein (APP) or presenilin mutations and the remarkable effect of Aβ elimination by its vaccine on AD phenotype. The suggested mechanism for Aβ accumulation in sporadic AD includes elevated generation of Aβ due to increased β-secretase activity (1), decreased degradation of Aβ (2), and decreased efflux of Aβ from the brain to blood (3).

Increased oxidative stress of brain is a key feature of sporadic AD and manifests predominantly as lipid peroxidation (4). There are several lines of evidence suggesting that the AD brain displays extensive oxidative damage to various biological macromolecules, including lipids, proteins, and nucleic acids (5). Both Aβ level and lipid peroxidation in the brain are increased with disease progression of AD. However, the direct relationship between Aβ accumulation and lipid peroxidation is unclear (6).

Among natural isomers of vitamin E, α-tocopherol (α-Toc) has the most potent biological activity and is a major antioxidant that protects polyunsaturated fatty acids from peroxidation. Brain α-Toc content is maintained by α-tocopherol transfer protein (α-TTP), which transfers α-Toc from chylomicron to very low-density lipoprotein in the liver and transports α-Toc from blood to brain (7, 8). We have developed an α-tocopherol transfer protein knock-out (*Ttpa*$^{-/-}$) mouse that showed marked lipid peroxidation because of a lack of α-Toc in the brain and considered it as a model for chronic oxidative stress to the brain (7). In a *Ttpa*$^{-/-}$ mouse brain, two lipid peroxidation markers, thiobarbituric acid reactive substrates

* This work was supported in part by a grant for Research on Psychiatric and Neurological Disease and Mental Health from the Ministry of Health, Labor, and Welfare of Japan (to T. Y. and H. M.), a grant from the 21st Century COE Program on Brain Integration and Its Disorders to Tokyo Medical and Dental University (to Y. N., H. S., and H. M.), a grant from the Ministry of Education, Science, and Culture (to N. I., H. T., T. Y., and H. T.), and a grant of the SORST of Japan Science and Technology Agency (to S. O. and T. Terasaki).

[S] The on-line version of this article (available at http://www.jbc.org) contains supplemental Tables 1–3.

[1] To whom correspondence should be addressed. Tel.: 81-3-5803-5234; Fax: 81-3-5803-0169; E-mail: tak-yokota.nuro@tmd.ac.jp.

[2] The abbreviations used are: Aβ, amyloid β; AD, Alzheimer disease; APP, β-amyloid precursor protein; α-TTP, α-tocopherol transfer protein; PBS, phosphate-buffered saline; BBB, blood-brain barrier; LRP-1, lipoprotein receptor-related protein-1; Pgp, p-glycoprotein; GLUT-1, glucose transporter-1; TTR, transthyretin; BEI, brain efflux index; CLtot, total body clearance; α-Toc, α-tocopherol; TBS, Tris-buffered saline; PIPES, 1,4-piperazinediethanesulfonic acid; CHAPS, 3-[(3-cholamidopropyl)dimethylammonio]-1-propanesulfonic acid; IDE, insulin-degrading enzyme.

and 4-hydroxynonenal, were increased, and lipofuscin was massively accumulated (7). It is of note that the same markers were elevated in AD brains (9–11). We previously crossed the AD transgenic (*APPsw*) model mouse (Tg2576) with *Ttpa*$^{-/-}$ mouse, and the resulting double-mutant (*Ttpa*$^{-/-}$*APPsw*) mouse showed earlier and more severe cognitive dysfunction and had increased amyloid plaques in the brain by depletion of α-Toc (12). As a next step, we have studied the mechanism of how chronic lipid peroxidation increased Aβ deposits. The studies of the lifecycle of Aβ from its generation to its metabolism have received an extraordinary amount of attention in the field of AD research. Although the Aβ level in the brain is determined by the rate of Aβ generation and clearance in the brain, the clearance of Aβ from circulation is also important for the Aβ accumulation in the brain, because the Aβ levels in the brain and in the blood are held in equilibrium (3). Therefore, we evaluated the Aβ generation in the brain and its clearance from the brain and from the blood in *Ttpa*$^{-/-}$ mouse. We also measured the aggregation capacity of Aβ in the brain to evaluate the effect of oxidative stress on the accumulation of Aβ in the brain.

EXPERIMENTAL PROCEDURES

Animals

All experiments were approved by the Animal Experiment Committees of Tokyo Medical and Dental University. We used *Ttpa*$^{-/-}$ mice from a C57BL/6J background (7). We crossbred *Ttpa*$^{-/-}$ mice with *APPsw* transgene hemizygous mice (Tg2576 from a C57BL/6-SJL background, Taconic, Hudson, NY), which is an AD model that overexpresses a human APP_{695} with a double mutation (*APPsw*; K670N,M671L) (13). We then cross-bred *Ttpa*$^{+/-}$*APPsw* and *Ttpa*$^{+/-}$ to produce the *Ttpa*$^{-/-}$*APPsw* mice. Animals were screened for the presence of APPsw and α-TTP genes by PCR analysis of tail DNA. Complete elimination of α-Toc from the brain is achieved only when the deletion of α-TTP gene is combined with the dietary restriction, because a part of α-Toc taken up from the small intestine can enter the brain even without α-TTP (7). Furthermore, it is impossible to produce mice with α-Toc-deficient diet because supplementation of α-Toc is necessary for the maintenance of pregnancy (7). The dietary restriction of α-Toc after birth could not eliminate α-Toc from the brain of wild-type mice (7). Therefore, to study the effect of α-Toc depletion on AD phenotype, we fed the resulting double mutant (*Ttpa*$^{-/-}$*APPsw*) mice on α-Toc-deficient diet (Funabashi Farm, Chiba, Japan) and compared with the *APPsw* littermate mice on normal diet (36 mg of α-Toc/kg). To determine whether the differences in the phenotypes between *APPsw* mice and *Ttpa*$^{-/-}$*APPsw* mice are caused by the *Ttpa*$^{-/-}$ gene effect or α-Toc-deficient effect, we furthermore made a group of *Ttpa*$^{-/-}$*APPsw* mice that were fed on α-Toc-supplemented diet (750 mg of α-Toc/kg, Funabashi Farm). Details for these diets were previously described (7). All mice were housed in plastic cages, received food and water *ad libitum*, and were maintained on a 12/12-h light-dark cycle (lights on at 09:00, off at 21:00).

Aβ Quantitation in the Brain and Plasma

Three or four 18-month-old mice for each group were anesthetized with an intraperitoneal injection of pentobarbital (60 mg/kg). After blood was collected, they killed by transcardiac perfusion with 0.01 M phosphate-buffered saline (PBS), pH 7.4. The cerebral hemisphere was homogenized in 50 mM Tris-HCl buffer (TBS), pH 7.6, containing 150 mM NaCl and a protease inhibitor mixture (Complete, Roche Diagnostics) supplemented with 0.7 μg/ml pepstatin A (Peptide Institute, Osaka, Japan) with a Teflon glass homogenizer and centrifuged at 200,000 × *g* for 20 min at 4 °C. The supernatant was defined as the TBS-soluble fraction. The pellet was solubilized by sonication in 6 M guanidine-HCl buffer containing a protease inhibitor mixture. The solubilized pellet was centrifuged as before, after which the supernatant was diluted 12-fold to reduce the concentration of guanidine-HCl and used as the TBS-insoluble fraction (guanidine-extractable). The amounts of $Aβ_{1-40}$ and $Aβ_{1-42}$ in each fraction and plasma were assayed using commercially available human $Aβ_{1-40}$ and $Aβ_{1-42}$ sandwich enzyme-linked immunosorbent assay kits (BioSource International, Inc., Camarillo, CA).

Northern Blot Analysis

Three or four 18-month-old mice in each group were examined. Total RNA was extracted from the brain by TRIzol (Invitrogen). Total RNA (2.5 μg) was fractionated in a formaldehyde-agarose gel and transferred to a Nytran membrane (Schleicher & Schuell). The upper part of the membrane was hybridized with a purified PCR fragment corresponding to human APPsw cDNA (bases 981–1578). The lower part was hybridized with a probe specific for glyceraldehyde-3-phosphate dehydrogenase to confirm the quantity of loaded RNA. The signals were visualized with a Gene Images CDP-star detection kit (Amersham Biosciences).

Western Blot Analysis

C-terminal Fragments of APP-β, -α, and -γ/ϵ—Three or four 18-month-old mice in each group were examined. To analyze C-terminal fragments -β, -α, and -γ/ϵ, the cerebral hemisphere was homogenized with 50 mM TBS and centrifuged at 800 × *g* for 10 min at 4 °C. The supernatant was centrifuged at 200,000 × *g* for 28 min at 4 °C, and the resultant pellet was resuspended with 20 mM PIPES, pH 7.0, containing 140 mM KCl, 0.25 M sucrose, 5 mM EGTA, and a protease inhibitor mixture. Protein concentration was determined using a BCA protein assay kit (Pierce) and adjusted. After incubation of the suspension at 37 °C for 60 min, it was delipidized with chloroform:methanol (2:1) and chloroform:methanol:distilled water (1:2:0.8) sequentially to improve sensitivity. The resultant protein fraction was dried by evaporation and then solubilized with a sample buffer containing 9 M urea. Samples (20 μg) were separated by 16.5% SDS-polyacrylamide gel electrophoresis and transferred electrophoretically to nitrocellulose membranes (Schleicher & Schuell). The membranes were boiled in PBS for 3 min to improve sensitivity. The blot was probed with the rabbit polyclonal antibody against the C terminus of APP (A8717, Sigma) followed by the avidin-biotin-peroxidase complex (ABC) method (Vectastain ABC kits, Vector Laboratories,

Burlingame, CA). The immunoreactive band on the membrane was visualized with a Supersignal West Pico Chemiluminescence kit (Pierce).

Proteins to Transport Aβ across the Blood-Brain Barrier (BBB)—Three sets of three 8-month-old mice in each group were examined. The vascular fraction of small vessels was prepared from whole cerebrum using a modified method reported previously (14). Briefly, brains were homogenized in 10 mM PBS. After centrifugation at 800 × *g* for 5 min at 4 °C, the pellets were suspended with a dextran solution (M_r 70,000; 15% w/v, Sigma) and centrifuged at 4500 × *g* for 10 min at 4 °C. The pellets were washed by 10 mM PBS twice and resuspended with 5 mM PBS for 10 min. After centrifuging at 800 × *g* for 5 min, the final pellets of small vessels were resuspended by pipetting and vortexed in the homogenization buffer containing 10 mM TBS, pH 7.4, containing 1 mM EDTA, 150 mM NaCl, 4% CHAPS, 1 mM phenylmethylsulfonyl fluoride, and a protease-inhibitor mixture (Complete-Mini, Roche Diagnostics). The 4.5-μg samples were separated by 7.5 and 15% SDS-polyacrylamide mini-gel and transferred to a nitrocellulose membrane. The membrane was probed with mouse anti-low density lipoprotein receptor-related protein-1 (LRP-1) (β-chain specific, American Diagnostica Inc., Stamford, CT) or mouse anti-p-glycoprotein (Pgp) (C219, Signet, Dedham, MA) followed by sheep anti-mouse secondary antibody conjugated to horseradish peroxidase (Amersham Biosciences). Rabbit anti-brain-type glucose transporter-1 (GLUT-1) antibody (Alpha Diagnostic International, San Antonio, TX) with donkey anti-rabbit secondary antibody (Amersham Biosciences) was also used. Bands were visualized by using an ECL Plus Western blotting system (Amersham Biosciences).

Protein to Transport Aβ into the Liver—Three 8-month-old mice in each group were examined. To prepare the crude membrane fraction, liver was homogenized in hypotonic lysis buffer (10 mM Tris, 10 mM NaCl, 1.5 mM $MgCl_2$, pH 7.4) with 1 mM phenylmethylsulfonyl fluoride and a protease-inhibitor mixture (Complete-Mini). After centrifugation at 8000 × *g* for 10 min at 4 °C, the supernatant was centrifuged at 100,000 × *g* for 60 min at 4 °C. The pellet obtained was regarded as the crude membrane fraction. Furthermore, to prepare the plasma membrane fraction of the liver, this obtained pellet was resuspended in 10 mM HEPES, 250 mM sucrose, pH 7.4, and overlaid on 38% sucrose solution and then centrifuged at 100,000 × *g* for 40 min at 4 °C using a swing rotor (SW40Ti; Beckman, Fullerton, CA). The turbid layer was collected and centrifuged at 100,000 × *g* for 1 h at 4 °C, and the obtained pellet was defined as plasma membrane fraction. The 2.5-μg samples were separated with 7.5% SDS-polyacrylamide mini-gel and transferred electrophoretically to a nitrocellulose membrane. The membrane was probed with mouse anti-LRP-1, rabbit anti-cadherin (ab16505, Abcam, Cambridge, UK), or mouse anti-β-actin (A2228, Sigma) followed by sheep anti-mouse secondary antibody conjugated to horseradish peroxidase or a goat anti-rabbit antibody (Pierce), respectively. Bands were visualized by using an ECL Plus Western blotting system or a Supersignal West Femto Maximum Sensitivity kit (Pierce).

Aβ Ligand Proteins in the Plasma—Three or four 14-month-old mice in each group were examined. The collected plasma was diluted with saline, and the 0.10-μl anti-apolipoprotein E (apoE) or 0.40-μl anti-transthyretin (TTR) samples were separated with 15% SDS-polyacrylamide mini-gel and transferred electrophoretically to a polyvinylidene difluoride membrane (Bio-Rad). The membrane was probed with goat polyclonal anti-apoE (sc-6384, Santa Cruz Biotechnology, Inc., Santa Cruz, CA) or rabbit anti-TTR (Dako, Glostrup, Denmark) followed by donkey anti-goat secondary antibody conjugated to horseradish peroxidase (Santa Cruz Biotechnology) or donkey anti-rabbit antibody (Amersham Biosciences). Bands were visualized by using an ECL Plus Western blotting system.

Aβ Degrading Proteins in the Brain—Three or five 23-month-old mice in each group were examined. The cerebral hemisphere was homogenized in homogenization buffer (0.1 M Tris-HCl, pH 8.0, 0.15 M NaCl, 1 mg/ml leupeptin, and 1 mg/ml pepstatin A) and centrifuged at 500 × *g* for 5 min. Membranes were prepared by precipitation of the postnuclear supernatant at 100,000 × *g* for 60 min. The resulting pellet was subjected to protein extraction using 2% SDS by homogenization and posterior centrifugation at 100,000 × *g* for 60 min at 4 °C. The supernatant was used as a membrane fraction. Protein concentration was determined using a BCA protein assay kit, and the membrane fraction (2.5 μg) was separated by 7.5% SDS-polyacrylamide gel electrophoresis and transferred electrophoretically to polyvinylidene difluoride membrane. The blotted membrane was probed with rabbit polyclonal anti-insulin-degrading enzyme (IDE) (Calbiochem) or mouse anti-flotillin (BD Biosciences) followed by donkey anti-rabbit or sheep anti-mouse secondary antibody conjugated to horseradish peroxidase (Amersham Biosciences). Bands were visualized by using an ECL Plus Western blotting system.

β- and γ-Secretase Activities Measurement

The total activities of β- and γ-secretase present in the cerebrum of four 9-month-old mice were determined using secretase-kits (R&D Systems, Wiesbaden, Germany) (15). Secretase enzymatic activities were proportional to the fluorometric reaction, and the data were corrected by subtraction of background control (reactions in the absence of tissue).

Study of Aβ Efflux from the Brain at the BBB

In vivo brain elimination experiments were performed using intracerebral microinjection as described previously (16, 17). Four 2- or 14-month-old mice in each group were anesthetized intramuscularly with a mixture of ketamine (125 mg/kg) and xylazine (1.22 mg/kg), then mounted on a stereotaxic frame (SRS-6, Narishige, Tokyo, Japan) to hold the heads in position. Using a dental drill, a bore hole was made 3.8 mm lateral to the bregma. Then extracellular fluid buffer (122 mM NaCl, 25 mM $NaHCO_3$, 3 mM KCl, 1.4 mM $CaCl_2$, 1.2 mM $MgSO_4$, 0.4 mM K_2HPO_4, 10 mM D-glucose, and 10 mM HEPES, pH 7.4) containing 0.012 μCi of ^{125}I-Aβ_{1-40} and 0.12 μCi of [^{3}H]dextran was injected over a period of 1 min using a 5.0-μl microsyringe (Hamilton, Reno, NE) fitted with a fine needle at a depth of 2.5 mm from the surface of the scalp, *i.e.* in the secondary somatosensory cortex 2 (S2) region. The needle was left in this configuration for an additional 4 min to prevent reflux of the injected solution along the injection track before being slowly retracted.

At the designated times after microinjection, aliquots of cerebrospinal fluid were collected from the cisterna magna as reported previously (17). The whole brain was subsequently removed, and the left cerebrum, right cerebrum, and cerebellum were isolated and dissolved in 2.0 ml of 2 M NaOH at 60 °C for 1 h. The ^{125}I radioactivity of the samples was measured in a γ-counter (ART300, Aloka, Tokyo, Japan) for 3 min. The samples were then mixed with 14 ml of Hionic-fluor (Packard Instrument Co.), and ^{3}H radioactivity was measured in a liquid scintillation counter (TRI-CARB2050CA, Packard Instrument Co.) for 5 min. No radioactivity associated with this efflux transport process was detected in the contralateral cerebrum, cerebellum, or cerebrospinal fluid (data not shown), suggesting the operation of a selective efflux transport process across the BBB. The brain efflux index (BEI) was defined by the equation BEI % = (test substrate undergoing efflux at the BBB)/(test substrate injected into the brain) × 100, and the percentage of substrate remaining in the ipsilateral cerebrum was determined from 100 − BEI (%) = (amount of test substrate in the brain/amount of reference in the brain)/(amount of test substrate injected/amount of injected as a reference in the brain) × 100. The apparent elimination rate constant (k_e) was determined from the slope given by fitting a semilogarithmic plot of 100 − BEI *versus* time using the nonlinear least-squares regression analysis program MULTI (18).

^{125}I-Aβ$_{1-40}$ Plasma Pharmacokinetic Studies

Four or five 2- and 25-month-old mice in each group were anesthetized intramuscularly with a mixture of ketamine (125 mg/kg) and xylazine (1.22 mg/kg), and the jugular vein was isolated. Their body temperature was kept at 37 °C on a hot plate. Each mouse received a bolus intravenous injection of ^{125}I-Aβ$_{1-40}$ (5 μCi; 100 μl) into the jugular vein. Blood samples (30 μl) were collected from the tail vein by using a heparinized microcapillary at various intervals (1, 3, 5, 10, 15, 30, 60, 120, and 360 min) after the injection. The blood samples were centrifuged at 10,000 × *g* for 5 min at 4 °C, and the supernatant was obtained. To assess the integrity of the peptides, a plasma aliquot at each time point was cold-precipitated with 10% trichloroacetic acid in saline. After trichloroacetic acid precipitation, the precipitant was dissolved in 200 μl of 2 M NaOH at 55 °C for 10 min. The ^{125}I radioactivity of the samples was measured in a γ-counter (ART300) for 3 min.

The plasma concentration *versus* time data were analyzed by MOMENT (19) based on the model-independent moment analysis method (20). Briefly, the area under the plasma concentration-time curve (AUC) extrapolated to infinity was calculated the equation AUC = $AUC_{0-360} + C_{360}/k_e$, in which AUC_{0-360} is the area under the curve from time 0 to the time of the last plasma sample at 360 min calculated by the log-trapezoidal method, C_{360} is plasma concentration of the last plasma sample at 360 min, and k_e is the terminal elimination rate constant estimated from terminal points using the Akaike's Information Criterion-based method. The total body clearance (CLtot) was calculated by the equation CLtot = dose/AUC, where dose is the administered amount of ^{125}I-Aβ$_{1-40}$. The mean residence time (MRT) and the steady-state volume of distribution (Vdss) were calculated by MRT = AUMC/AUC and Vdss = CL·MRT, where AUMC is the total area under the first-moment time curve extrapolated to infinity.

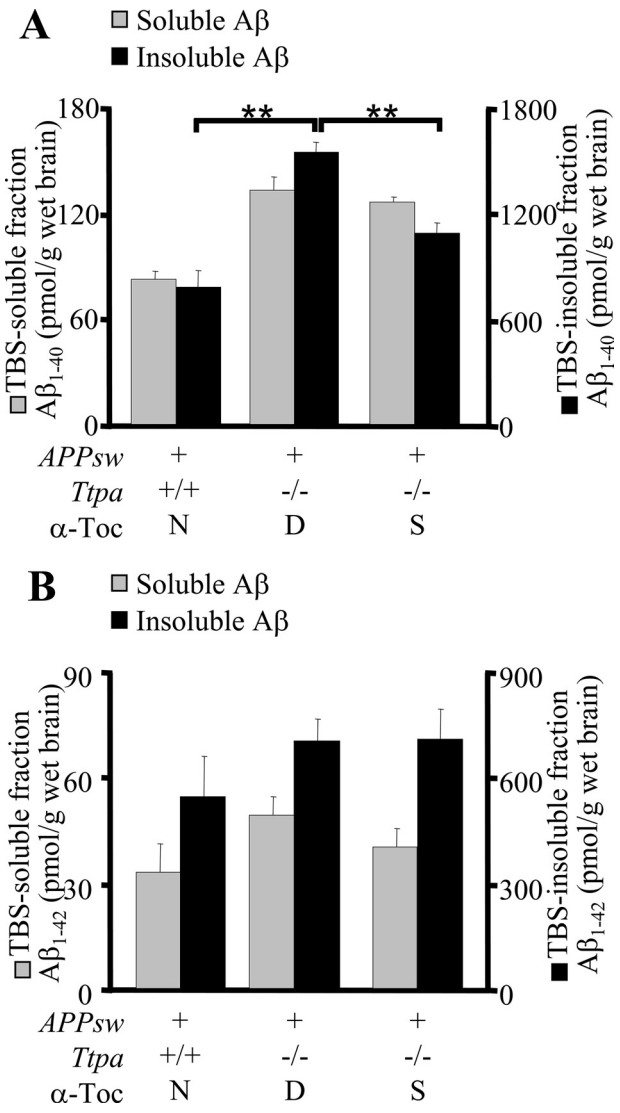

FIGURE 1. **The *Ttpa*$^{-/-}$*APPsw* mouse shows enhanced accumulation of Aβ in the brain.** *A* and *B*, cerebral Aβ$_{1-40}$ (*A*) and Aβ$_{1-42}$ (*B*) levels in 18-month-old mice. *Ttpa*$^{-/-}$*APPsw* mice showed increased level of Aβ$_{1-40}$ in the TBS-insoluble fraction of the brain homogenate and a similar tendency of increase of Aβ$_{1-40}$ and Aβ$_{1-42}$ in other fractions. This increase was partially ameliorated by α-Toc supplementation in the diet. *D*, α-Toc-deficient diet; *S*, α-Toc-supplemented diet; *N*, normal diet. **, $p < 0.01$.

Assay of Neprilysin-dependent Neutral Endopeptidase Activity

Four 4-month-old mice in each group were examined. Triton X-100-solubilized membrane fraction from brain was prepared to assay neutral endopeptidase activity as described previously (21). The neprilysin-dependent neutral endopeptidase activity was fluorometrically assayed using 0.1 mM succinyl-Ala-Ala-Phe-amidomethylcoumarin (Bachem, Bubendorf, Switzerland) as a substrate and determined from the fluorescence intensity (excitation, 390 nm; emission, 460 nm), based on the decrease in the rate of digestion caused by 0.1 μM thiorphan, a specific inhibitor of neprilysin.

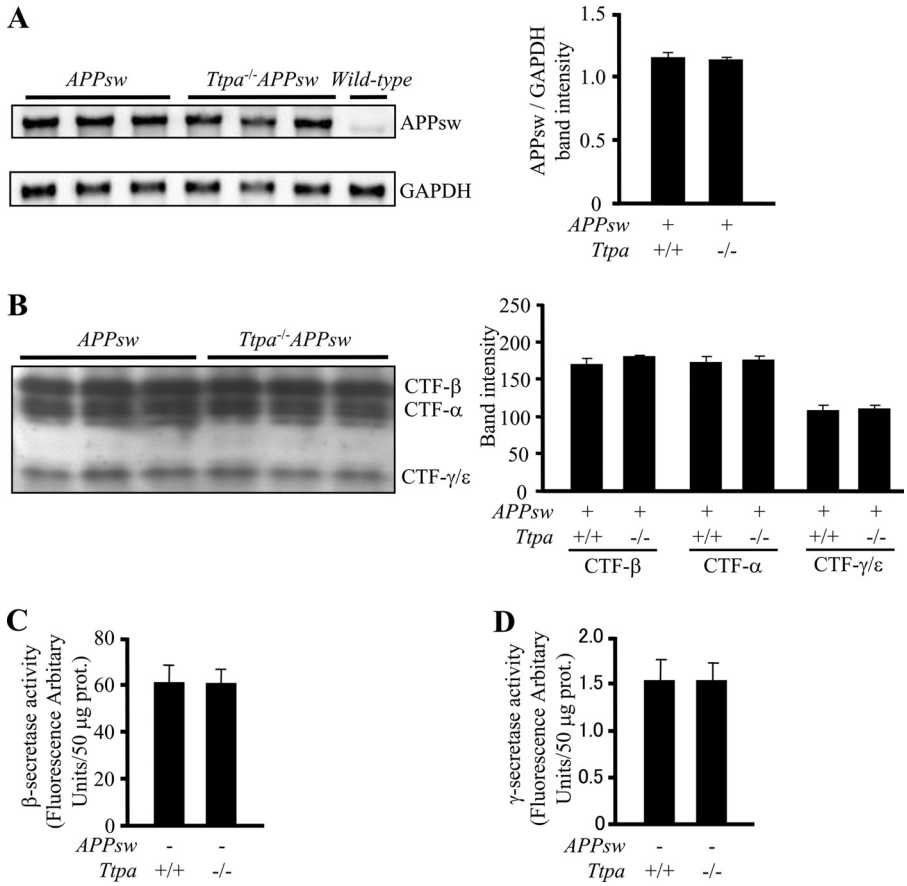

FIGURE 2. **α-Toc depletion does not increase APP expression nor β/γ-cleavages.** *A*, the human APPsw mRNA expression did not increase in the brains of *Ttpa*$^{-/-}$*APPsw* mice compared with *APPsw* mice. The band intensities normalized to the mouse glyceraldehyde-3-phosphate dehydrogenase (*GAPDH*) bands are shown in the *right panel*. *B*, protein levels of C-terminal fragments of APP-β, -α, and -γ/ε did not change in the brains of *Ttpa*$^{-/-}$*APPsw* mice compared with *APPsw* mice. Band intensities are shown in the *right panel*. *C* and *D*, the β (*C*)- and γ (*D*)-secretase activities did not increase in the brains of *Ttpa*$^{-/-}$ mice compared with wild-type mice.

Aβ Aggregation Study

Five 15-month-old *Ttpa*$^{-/-}$ mice and 10 age-matched wild-type mice were examined. Synaptosomes were prepared from mouse cerebrums as previously reported (22). Seed-free solutions of $A\beta_{1-40}$ were diluted with TBS. Aβ solutions at 50 μM were incubated at 37 °C with or without synaptosomes. Thioflavin T fluorescence intensities in the mixture incubated for 24 h were determined as previously described (23, 24).

Data Analysis

All data represent the average ± S.E. For multiple comparisons, single-factor analysis of variance followed by Fisher's protected least-significant-difference post hoc test was used. Results were considered statistically significant at $p < 0.05$.

RESULTS

Ttpa$^{-/-}$*APPsw Mouse Has an Enhanced Accumulation of Aβ in the Brain*—First, we biochemically studied the effect of α-Toc depletion on accumulation of Aβ. At 18 months, *Ttpa*$^{-/-}$*APPsw* mice showed markedly increased levels of $A\beta_{1-40}$ in the TBS-insoluble fraction of the brain homogenate and a similar tendency of increase of $A\beta_{1-40}$ and $A\beta_{1-42}$ in other fractions (Fig. 1, *A* and *B*). The *in vivo* accumulation of $A\beta_{1-40}$ was decreased when *Ttpa*$^{-/-}$*APPsw* mice were fed on the α-Toc-supplemented diet (Fig. 1*A*). An incomplete effect of α-Toc supplementation on accumulation of Aβ might be explained by the poor recruitment of supplemented α-Toc into the brain in *Ttpa*$^{-/-}$*APPsw* mice, because α-TTP in the brain transports α-Toc from blood to brain (7). This partial effect of α-Toc supplementation still could reduce accumulation of Aβ plaques (12).

APP Expression and β/γ Cleavages Are Not Increased—To examine the effect of α-Toc depletion on the metabolism of Aβ, we evaluated Aβ generation by measuring APP expression and secretase activities. The mRNA level of human APPsw in the brain did not increase in the brains of *Ttpa*$^{-/-}$*APPsw* mice compared with *APPsw* mice at 18 months of age (Fig. 2*A*). Moreover, protein levels of C-terminal fragments of APP-β, -α, and -γ/ε did not change in the brains of *Ttpa*$^{-/-}$*APPsw* mice compared with *APPsw* mice (Fig. 2*B*). This was supported by the *in vitro* results that β- and γ-secretase activities were not increased in the brains of 9-month-old *Ttpa*$^{-/-}$ mice (Fig. 2, *C* and *D*). These results indicate that the generation of Aβ in the brain of *Ttpa*$^{-/-}$*APPsw* mouse is not influenced by the depletion of α-Toc.

Aβ Clearance from the Brain Is Decreased in Ttpa$^{-/-}$ *Mice*—The increased Aβ accumulation without change of Aβ generation in *Ttpa*$^{-/-}$*APPsw* mouse brain led us to postulate that the increased Aβ accumulation by lipid peroxidation occurs through decreased Aβ clearance from the brain. Then we next directly studied Aβ clearance from the brain *in vivo* by using the BEI method (16, 17). We used *Ttpa*$^{-/-}$ mice in this experiment, because the injected ^{125}I-$A\beta_{1-40}$ should have been competed with endogenous Aβ, which accumulated in different degree in *Ttpa*$^{-/-}$*APPsw* and *APPsw* mouse brains, thereby complicating interpretation of the results. In contrast, *Ttpa*$^{-/-}$ mice have no detectable endogenous mouse Aβ in the brain. The ^{125}I-$A\beta_{1-40}$ was microinjected into the mouse cerebral cortex, and the remaining ^{125}I-$A\beta_{1-40}$ levels in the ipsilateral cerebrum were measured. The percentage of ^{125}I-$A\beta_{1-40}$ remaining at 60 min after injection was increased in 14-month-old *Ttpa*$^{-/-}$ mice compared with age-matched wild-type mice (Fig. 3*A*). The apparent elimination rate constant (k_e) was also markedly decreased because of α-Toc depletion (Fig. 3*B*). Although Aβ clearance decreases as a consequence of normal aging (25, 26), the reduction in k_e value evoked by α-Toc depletion (27.7%) was

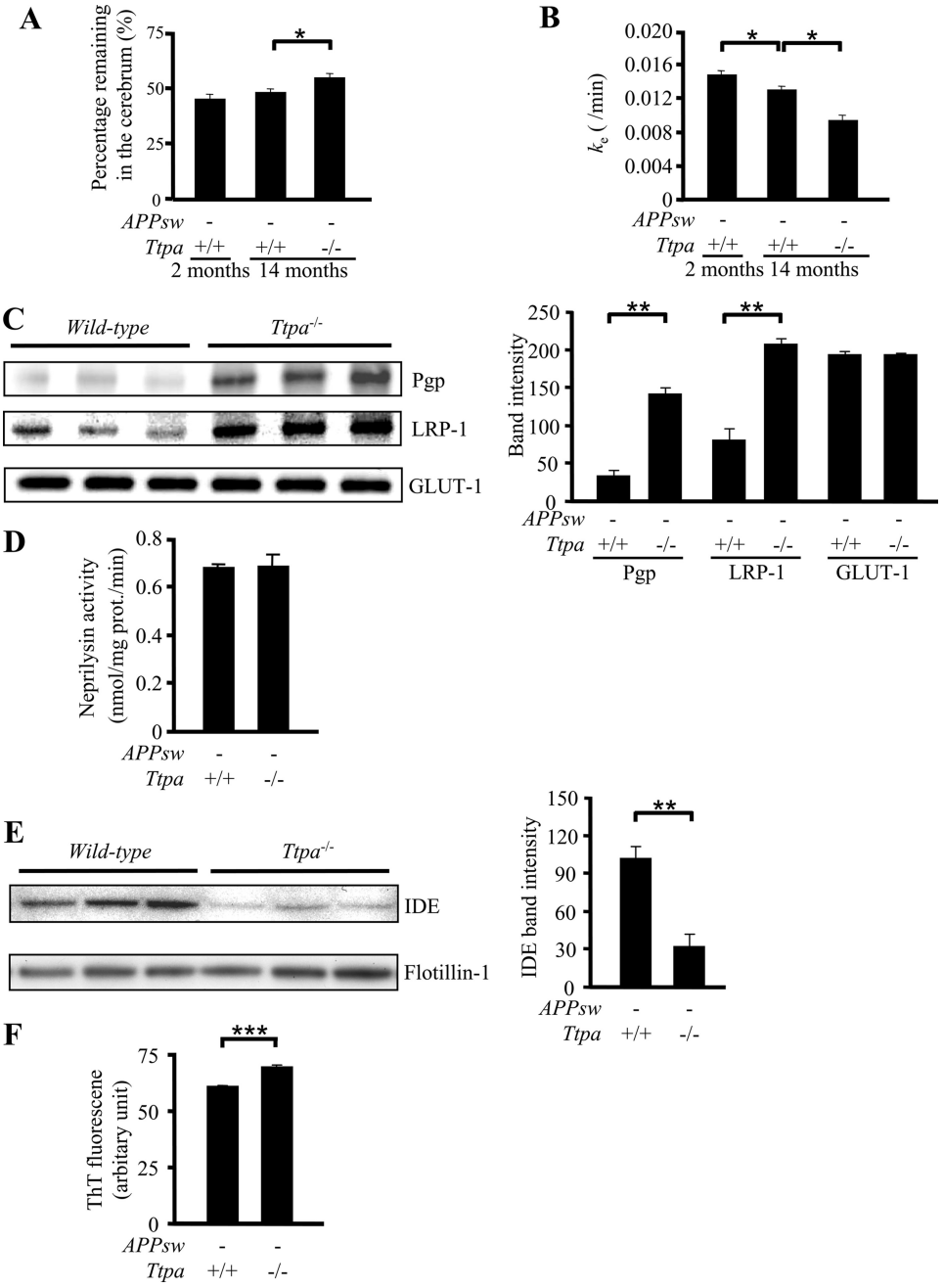

FIGURE 3. **α-Toc depletion decreases Aβ clearance.** *A*, the remaining percentage of ^{125}I-Aβ_{1-40} at 60 min was higher in 14-month-old *Ttpa*$^{-/-}$ mice than in age-matched wild-type mice. *B*, k_e was markedly decreased in *Ttpa*$^{-/-}$ mice. *C*, protein levels of LRP-1 and Pgp were increased in the brains of *Ttpa*$^{-/-}$ mice compared with wild-type mice, whereas levels of GLUT-1 were not changed between them. Band intensities are shown in the *right panel*. *D*, neprilysin-dependent endopeptidase activity did not decrease in *Ttpa*$^{-/-}$ mice compared with wild-type mice. *E*, protein levels of IDE were decreased in the brains of *Ttpa*$^{-/-}$ mice compared with wild-type mice. Band intensities are shown in the *right panel*. *F*, thioflavin T (*ThT*) fluorescence intensity in the incubation mixtures of synaptosomes with synthetic Aβ_{1-40} was increased in the brains of *Ttpa*$^{-/-}$ mice compared with wild-type mice. *, $p < 0.05$; **, $p < 0.01$; ***, $p < 0.0001$.

much greater than that by aging, as shown between 2 and 14 months of age (13.4%). One of the most likely pathologies influencing Aβ clearance is the compromised BBB by oxidative stress with vitamin E deficiency. However, there is no evidence of abnormal structures of endothelial cells or ischemic change on histological analysis of the *Ttpa*$^{-/-}$ mouse brains (data not shown).

Efflux Transporters for Aβ across the BBB Are Up-regulated in the Brain Capillary Endothelial Cells of Ttpa$^{-/-}$ *Mouse*—One of possible causes of impaired Aβ clearance is the decreased efflux and the decreased degradation of Aβ. To examine whether reported molecules involved in Aβ transport at the BBB were down-regulated, we measured the protein levels of LRP-1 and Pgp. Surprisingly, both protein levels in the small vascular fraction in the brains of *Ttpa*$^{-/-}$ mice were much increased compared with wild-type mice (Fig. 3*C*). In contrast, there was no change in the levels of GLUT-1, which is a transporter localized to the brain capillary endothelial cells (27).

Aβ-degrading Peptidase, IDE, Is Decreased in Ttpa$^{-/-}$ *Mouse Brain*—Next, we studied Aβ-degrading peptidases, neprilysin and IDE, for studying another possible cause of impaired Aβ clearance. Although the enzymatic activity of neprilysin was not decreased in *Ttpa*$^{-/-}$ mouse brain compared with wild-type mouse (Fig. 3*D*), expression level of IDE was markedly decreased in *Ttpa*$^{-/-}$ mouse brain (Fig. 3*E*). We, therefore, consider that an impaired degradation of Aβ in the brain because of decreased IDE is related with enhanced Aβ accumulation in *Ttpa*$^{-/-}$*APPsw* mouse brain.

Aβ Aggregation Is Accelerated in Ttpa$^{-/-}$ *Mouse Brains*—Moreover, we studied the effect of oxidative stress on Aβ aggregation capacity. The aggregation of Aβ_{1-40} in the presence of synaptosomes was measured by using thioflavin T fluorescence. The aggregation capacity was increased in brain homogenates of the *Ttpa*$^{-/-}$ mice compared with wild-type homogenates (Fig. 3*F*).

Ttpa$^{-/-}$*APPsw Mouse Has an Increased Level of Aβ in the Plasma as Well as in the Brain*—Furthermore, we measured the plasma levels of Aβ in *Ttpa*$^{-/-}$*APPsw* mouse. The 18-month-old *Ttpa*$^{-/-}$*APPsw* mice showed markedly increased levels of both plasma Aβ_{1-40} and Aβ_{1-42} (Fig. 4*A*). These accumulations of Aβ_{1-40} and Aβ_{1-42} were partially recovered when *Ttpa*$^{-/-}$*APPsw* mice were fed on the α-Toc-supplemented diet (Fig. 4*A*). In contrast, the Aβ-binding proteins in the plasma,

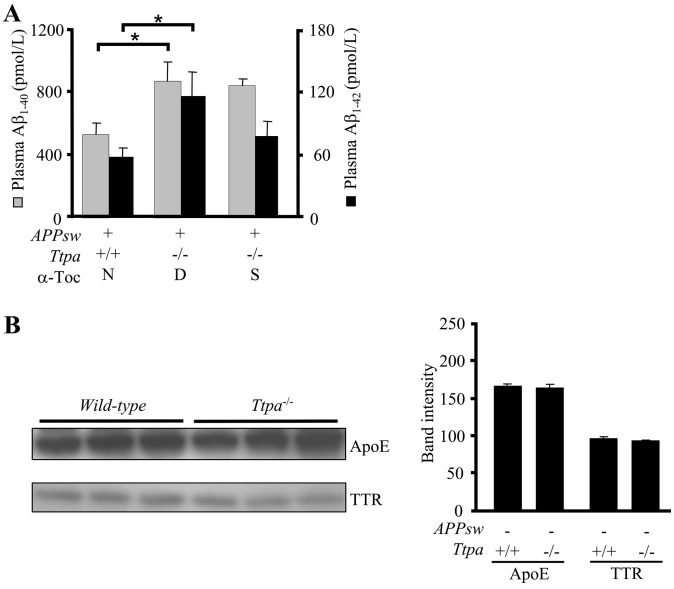

FIGURE 4. **The *Ttpa*$^{-/-}$*APPsw* mouse shows enhanced accumulation of Aβ in the plasma.** *A*, 18-month-old *Ttpa*$^{-/-}$*APPsw* mice showed increased levels of $A\beta_{1-40}$ and $A\beta_{1-42}$. This increase was partially ameliorated by α-Toc supplementation in the diet. *B*, protein levels of apoE and TTR were not changed in the plasma of *Ttpa*$^{-/-}$ mice compared with wild-type mice. Band intensities are shown in the *right panel*. *D*, α-Toc-deficient diet; *S*, α-Toc-supplemented diet; *N*, normal diet. *, $p < 0.05$.

apoE, and TTR levels were not different between *Ttpa*$^{-/-}$ mice and wild-type mice (Fig. 4*B*).

Increased Aβ Accumulation in the Plasma Is also Caused by Impairment of Aβ Clearance from the Blood—The systemic clearance of Aβ should influence the levels of plasma Aβ. Therefore, the effect of *Ttpa* deficiency on systemic clearance of Aβ from the circulation was investigated *in vivo*. We also used *Ttpa*$^{-/-}$ in this experiment instead of *Ttpa*$^{-/-}$*APPsw* and *APPsw* mice, because the CLtot, a primary pharmacokinetic parameter that is a measure of the elimination efficiency of peripherally injected ^{125}I-$A\beta_{1-40}$, is known to decrease significantly in the presence of high plasma levels of $A\beta_{1-40}$ (28). Fig. 5*A* shows the plasma concentration-time profiles of trichloroacetic acid-precipitable ^{125}I-$A\beta_{1-40}$ after intravenous bolus administration in 2- and 25-month-old wild-type and 25-month-old *Ttpa*$^{-/-}$ mice. Plasma concentration of trichloroacetic acid-precipitable ^{125}I-$A\beta_{1-40}$ in 25-month-old *Ttpa*$^{-/-}$ mice was significantly greater at 1, 3, 60, and 360 min and substantially greater at all time points than that in 25-month-old wild-type mice (supplemental Table 1). As shown in supplemental Table 2, the AUC for *Ttpa*$^{-/-}$ mice was significantly greater than that for age-matched wild-type mice by 2.8-fold. To evaluate the systemic clearance more in detail, other pharmacokinetic parameters were determined and summarized in supplemental Table 2. In 25-month-old *Ttpa*$^{-/-}$ mice, CLtot and k_e (elimination rate constant) were significantly decreased by 41.2 and 51.7%, respectively, compared with those in age-matched wild-type mice (Fig. 5*B* and supplemental Table 2). The reduction in CLtot evoked by α-Toc depletion (41.2%) was much greater than that by aging, as shown between 2 and 25 months of age (14.1%) in model-independent moment analysis. The similar results were obtained in model dependent analysis as well (supplemental Table 2).

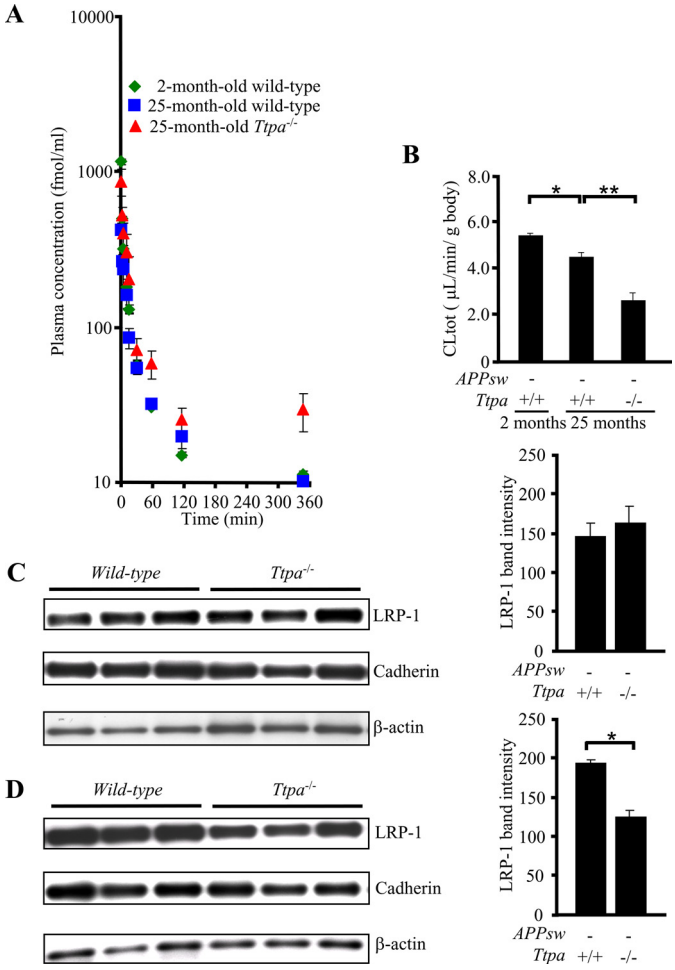

FIGURE 5. **α-Toc depletion decreases Aβ clearance from the plasma.** *A*, the remaining level of trichloroacetic acid-precipitable ^{125}I-$A\beta_{1-40}$ after its injection from the jugular vein was higher in 25-month-old *Ttpa*$^{-/-}$ mice than in wild-type mice. *B*, the total body clearance of ^{125}I-$A\beta_{1-40}$ was markedly decreased in *Ttpa*$^{-/-}$ mice compared with wild-type mice. *C* and *D*, the protein level of LRP-1 was decreased not in the crude membrane fraction of the liver of *Ttpa*$^{-/-}$ mice (*C*) but in the plasma membrane fraction (*D*) compared with wild-type mice. *, $p < 0.05$.

These results demonstrated that systemic clearance was attenuated in 25-month-old *Ttpa*$^{-/-}$ mice, and the decrease in the systemic clearance is likely to be because of a decrease in the clearance from the liver, as the systemic clearance of Aβ has been reported to be mostly mediated by clearance from the liver (29, 30).

LRP-1 Is Down-regulated in the Plasma Membrane Fraction of the Liver in Ttpa$^{-/-}$ *Mice*—To examine whether the Aβ receptor was down-regulated in the liver for the cause of impaired Aβ clearance from the blood, we measured the protein level of LRP-1 in the crude and plasma membrane fractions of the liver, as LRP-1 translocates from Golgi apparatus to plasma membrane in their activation for transporting Aβ into the hepatocytes (31). The protein level of LRP-1 was unchanged in the crude membrane fraction but decreased in the plasma membrane fraction of *Ttpa*$^{-/-}$ mouse liver (Fig. 5, *C* and *D*). This inactivation of LRP-1 might explain the decreased clearance of Aβ from the blood, causing increased Aβ in *Ttpa*$^{-/-}$*APPsw* mouse plasma.

DISCUSSION

We clearly demonstrated that Aβ clearances from the brain and from the blood were decreased in *Ttpa*$^{-/-}$ mice. Because the Aβ generation in *Ttpa*$^{-/-}$*APPsw* mouse brain was not increased, we consider that accumulated Aβ in *Ttpa*$^{-/-}$*APPsw* mouse brain is caused by these impaired Aβ clearances. The Aβ clearance from the brain can be accomplished via two major pathways; that is, receptor-mediated transport from the brain and proteolytic degradation in the brain. First, two proteins expressed in brain endothelial cells, LRP-1 and Pgp, are reported to regulate Aβ clearance by controlling its efflux from brain to blood based on the studies of genetically engineered mice (32, 33). Actually, LRP-1 was down-regulated in older mice, and this down-regulation correlated with Aβ accumulation in AD brains (25). Pgp expression was also inversely correlated with deposition of Aβ in the brains of elderly non-demented humans (34). Surprisingly, both LRP-1 and Pgp levels are markedly increased in *Ttpa*$^{-/-}$ mouse brains, although clearance of ^{125}I-Aβ_{1-40} by the BEI method is impaired. There are two possible explanations for the up-regulations of LRP-1 and Pgp. One is to compensate their dysfunctions, and another is to transport increased other substrates in the brain caused by lipid peroxidation. Second, the two major endopeptidases involved in proteolysis-related degradation of Aβ in the brain are neprilysin and IDE. Whereas the activity of neprilysin was not decreased, the protein level of IDE was markedly decreased in *Ttpa*$^{-/-}$ mouse brain. Furthermore, we made a gene chip analysis and evaluated all the molecules cyclopedically in the brains of *Ttpa*$^{-/-}$ and wild-type littermate mice. As a result, the only reasonable change of expression level for possibly causing enhanced Aβ accumulation was the decrease in IDE mRNA (supplemental Table 3, *A* and *B*). The homozygous deletion of IDE gene are known to show decreased Aβ degradation and increased accumulation of endogenous Aβ in the mouse brains (35, 36). Moreover, we previously confirmed that contribution of IDE to the clearance of microinjected ^{125}I-Aβ_{1-40} in the BEI method could be 25.3% by the pre-administration of IDE inhibitors, bacitracin (26). Together, as one of molecular mechanisms of Aβ accumulation and impaired clearance of Aβ in *Ttpa*$^{-/-}$*APPsw* mouse brains, we think that degradation of Aβ was impaired by decreased expression of IDE. However, we cannot exclude the possibility of dysfunction of other proteins because of lipid peroxidation, which may contribute to abnormal Aβ metabolism.

There are reports that AD patients showed increased levels of peripherally circulating Aβ (37, 38). In *Ttpa*$^{-/-}$*APPsw* mice as well, plasma Aβ levels are proved to be markedly increased to be compared with *APPsw* mice. Significantly lowered clearance of injected ^{125}I-Aβ_{1-40} from the *Ttpa*$^{-/-}$ mouse blood could explain the increased plasma Aβ in *Ttpa*$^{-/-}$*APPsw* mice. Although the excretion of Aβ through the kidney accounts only for a minute portion of Aβ in the blood (39), the liver is the major organ responsible for blood clearance of Aβ (29). We previously reported that LRP-1 in hepatocytes plays an important role to uptake plasma Aβ because mice with down-regulated LRP-1 by knock-out of receptor-associated protein or hydrodynamic injection of siRNA showed a much decreased uptake of ^{125}I-Aβ_{1-40} into the liver (40). The 85-kDa LRP-1 is proteolytically cleaved from a 600-kDa precursor in Golgi apparatus and is translocated by receptor-associated protein to plasma membrane to be activated for bounding Aβ (41). The result of decreased LRP-1 in the plasma membrane fraction without change of LRP-1 level in the crude membrane fraction of *Ttpa*$^{-/-}$ mouse liver indicated that lipid peroxidation does not affect LRP-1 expression itself but suggested a disturbed translocation of LRP-1. In another view, plasma Aβ level could be influenced by a change of its plasma ligands; apoE, TTR, and soluble LRP-1 (30, 42, 43). When soluble LRP-1 is oxidized, it is known to be decreased in its affinity to Aβ_{1-40} and Aβ_{1-42} (43). Although serum apoE and TTR levels in *Ttpa*$^{-/-}$ mice were not decreased, we could not evaluate serum soluble LRP-1 nor oxidized soluble LRP-1 level. Therefore, we cannot exclude the possibility that soluble LRP-1 is affected by the lipid peroxidation and causes the increased Aβ accumulation in *Ttpa*$^{-/-}$*APPsw* mouse plasma.

Given the fact that a large number of sporadic AD cannot be explained by increased Aβ generation (3), better understanding of the molecular and genetic basis of the Aβ clearance mechanisms may hold at least in part the key for research of AD pathology. A strongest risk factor for AD is aging (44), and lipid peroxidation may be a major cause for aging of the brain (45). In these respects, our findings of increased accumulation and aggregation of Aβ with impaired clearance due to lipid peroxidation are new aspects of AD pathology. We hope that further investigation on the molecular mechanism of impaired Aβ clearance due to lipid peroxidation provides a novel diagnostic and therapeutic target of AD.

Acknowledgments—We thank Hiroyuki Arai, Mikio Shoji, Akihiko Nunomura, and Masaki Nishimura for invaluable suggestions and discussion and Iichirou Oonishi for assistance.

REFERENCES

1. Li, R., Lindholm, K., Yang, L. B., Yue, X., Citron, M., Yan, R., Beach, T., Sue, L., Sabbagh, M., Cai, H., Wong, P., Price, D., and Shen, Y. (2004) *Proc. Natl. Acad. Sci. U.S.A.* **101,** 3632–3637
2. Iwata, N., Higuchi, M., and Saido, T. C. (2005) *Pharmacol. Ther.* **108,** 129–148
3. Zlokovic, B. V. (2004) *J. Neurochem.* **89,** 807–811
4. Barnham, K. J., Masters, C. L., and Bush, A. I. (2004) *Nat. Rev. Drug Discov.* **3,** 205–214
5. Moreira, P. I., Smith, M. A., Zhu, X., Nunomura, A., Castellani, R. J., and Perry, G. (2005) *Ann. N.Y. Acad. Sci.* **1043,** 545–552
6. Andersen, J. K. (2004) *Nat. Med.* **10,** S18–25
7. Yokota, T., Igarashi, K., Uchihara, T., Jishage, K., Tomita, H., Inaba, A., Li, Y., Arita, M., Suzuki, H., Mizusawa, H., and Arai, H. (2001) *Proc. Natl. Acad. Sci. U.S.A.* **98,** 15185–15190
8. Traber, M. G., Burton, G. W., and Hamilton, R. L. (2004) *Ann. N.Y. Acad. Sci.* **1031,** 1–12
9. Dowson, J. H., Mountjoy, C. Q., Cairns, M. R., and Wilton-Cox, H. (1992) *Neurobiol Aging* **13,** 493–500
10. Lovell, M. A., Ehmann, W. D., Butler, S. M., and Markesbery, W. R. (1995) *Neurology* **45,** 1594–1601
11. Sayre, L. M., Zelasko, D. A., Harris, P. L., Perry, G., Salomon, R. G., and Smith, M. A. (1997) *J. Neurochem.* **68,** 2092–2097
12. Nishida, Y., Yokota, T., Takahashi, T., Uchihara, T., Jishage, K., and Mizusawa, H. (2006) *Biochem. Biophys. Res. Commun.* **350,** 530–536
13. Hsiao, K., Chapman, P., Nilsen, S., Eckman, C., Harigaya, Y., Younkin, S.,

Yang, F., and Cole, G. (1996) *Science* **274,** 99–102
14. Kanda, T., Yoshino, H., Ariga, T., Yamawaki, M., and Yu, R. K. (1994) *J. Cell Biol.* **126,** 235–246
15. Apelt, J., Bigl, M., Wunderlich, P., and Schliebs, R. (2004) *Int. J. Dev. Neurosci.* **22,** 475–484
16. Kakee, A., Terasaki, T., and Sugiyama, Y. (1996) *J. Pharmacol. Exp. Ther.* **277,** 1550–1559
17. Hino, T., Yokota, T., Ito, S., Nishina, K., Kang, Y. S., Mori, S., Hori, S., Kanda, T., Terasaki, T., and Mizusawa, H. (2006) *Biochem. Biophys. Res. Commun.* **340,** 263–267
18. Yamaoka, K., Tanigawara, Y., Nakagawa, T., and Uno, T. (1981) *J. Pharmacobiodyn.* **4,** 879–885
19. Tabata, K., Yamaoka, K., Kaibara, A., Suzuki, S., Terakawa, M., and Hata, T. (1999) *Xenobiol. Metabol. Dispos.* **14,** 286–293
20. Yamaoka, K., Nakagawa, T., and Uno, T. (1978) *J. Pharmacokinet. Biopharm.* **6,** 547–558
21. Ogawa, T., Kiryu-Seo, S., Tanaka, M., Konishi, H., Iwata, N., Saido, T., Watanabe, Y., and Kiyama, H. (2005) *J. Neurochem.* **95,** 1156–1166
22. Igbavboa, U., Avdulov, N. A., Schroeder, F., and Wood, W. G. (1996) *J. Neurochem.* **66,** 1717–1725
23. Naiki, H., and Gejyo, F. (1999) *Methods Enzymol.* **309,** 305–318
24. Hayashi, H., Kimura, N., Yamaguchi, H., Hasegawa, K., Yokoseki, T., Shibata, M., Yamamoto, N., Michikawa, M., Yoshikawa, Y., Terao, K., Matsuzaki, K., Lemere, C. A., Selkoe, D. J., Naiki, H., and Yanagisawa, K. (2004) *J. Neurosci.* **24,** 4894–4902
25. Shibata, M., Yamada, S., Kumar, S. R., Calero, M., Bading, J., Frangione, B., Holtzman, D. M., Miller, C. A., Strickland, D. K., Ghiso, J., and Zlokovic, B. V. (2000) *J. Clin. Invest.* **106,** 1489–1499
26. Shiiki, T., Ohtsuki, S., Kurihara, A., Naganuma, H., Nishimura, K., Tachikawa, M., Hosoya, K., and Terasaki, T. (2004) *J. Neurosci.* **24,** 9632–9637
27. Pardridge, W. M., Boado, R. J., and Farrell, C. R. (1990) *J. Biol. Chem.* **265,** 18035–18040
28. Kandimalla, K. K., Curran, G. L., Holasek, S. S., Gilles, E. J., Wengenack, T. M., and Poduslo, J. F. (2005) *J. Pharmacol. Exp. Ther.* **313,** 1370–1378
29. Ghiso, J., Shayo, M., Calero, M., Ng, D., Tomidokoro, Y., Gandy, S., Rostagno, A., and Frangione, B. (2004) *J. Biol. Chem.* **279,** 45897–45908
30. Hone, E., Martins, I. J., Fonte, J., and Martins, R. N. (2003) *J. Alzheimers Dis.* **5,** 1–8
31. Tamaki, C., Ohtsuki, S., and Terasaki, T. (2007) *Mol. Pharmacol.* **72,** 850–855
32. Van, Uden, E., Mallory, M., Veinbergs, I., Alford, M., Rockenstein, E., and Masliah, E. (2002) *J. Neurosci.* **22,** 9298–9304
33. Cirrito, J. R., Deane, R., Fagan, A. M., Spinner, M. L., Parsadanian, M., Finn, M. B., Jiang, H., Prior, J. L., Sagare, A., Bales, K. R., Paul, S. M., Zlokovic, B. V., Piwnica-Worms, D., and Holtzman, D. M. (2005) *J. Clin. Invest.* **115,** 3285–3290
34. Vogelgesang, S., Cascorbi, I., Schroeder, E., Pahnke, J., Kroemer, H. K., Siegmund, W., Kunert-Keil, C., Walker, L. C., and Warzok, R. W. (2002) *Pharmacogenetics* **12,** 535–541
35. Farris, W., Mansourian, S., Chang, Y., Lindsley, L., Eckman, E. A., Frosch, M. P., Eckman, C. B., Tanzi, R. E., Selkoe, D. J., and Guenette, S. (2003) *Proc. Natl. Acad. Sci. U.S.A.* **100,** 4162–4167
36. Miller, B. C., Eckman, E. A., Sambamurti, K., Dobbs, N., Chow, K. M., Eckman, C. B., Hersh, L. B., and Thiele, D. L. (2003) *Proc. Natl. Acad. Sci. U.S.A.* **100,** 6221–6226
37. Kuo, Y. M., Emmerling, M. R., Lampert, H. C., Hempelman, S. R., Kokjohn, T. A., Woods, A. S., Cotter, R. J., and Roher, A. E. (1999) *Biochem. Biophys. Res. Commun.* **257,** 787–791
38. Matsubara, E., Ghiso, J., Frangione, B., Amari, M., Tomidokoro, Y., Ikeda, Y., Harigaya, Y., Okamoto, K., and Shoji, M. (1999) *Ann. Neurol.* **45,** 537–541
39. Ghiso, J., Calero, M., Matsubara, E., Governale, S., Chuba, J., Beavis, R., Wisniewski, T., and Frangione, B. (1997) *FEBS Lett.* **408,** 105–108
40. Tamaki, C., Ohtsuki, S., Iwatsubo, T., Hashimoto, T., Yamada, K., Yabuki, C., and Terasaki, T. (2006) *Pharm. Res.* **23,** 1407–1416
41. Willnow, T. E., Armstrong, S. A., Hammer, R. E., and Herz, J. (1995) *Proc. Natl. Acad. Sci. U.S.A.* **92,** 4537–4541
42. Matsubara, E., Sekijima, Y., Tokuda, T., Urakami, K., Amari, M., Shizuka-Ikeda, M., Tomidokoro, Y., Ikeda, M., Kawarabayashi, T., Harigaya, Y., Ikeda, S., Murakami, T., Abe, K., Otomo, E., Hirai, S., Frangione, B., Ghiso, J., and Shoji, M. (2004) *Neurobiol. Aging* **25,** 833–841
43. Sagare, A., Deane, R., Bell, R. D., Johnson, B., Hamm, K., Pendu, R., Marky, A., Lenting, P. J., Wu, Z., Zarcone, T., Goate, A., Mayo, K., Perlmutter, D., Coma, M., Zhong, Z., and Zlokovic, B. V. (2007) *Nat. Med.* **13,** 1029–1031
44. Katzman, R., and Saitoh, T. (1991) *FASEB J.* **5,** 278–286
45. Sohal, R. S., and Weindruch, R. (1996) *Science* **273,** 59–63